EFFECT OF COPPER (II) TOWARDS THE PHYSICAL AND CHEMICAL PROPERTIES OF VANADIUM PHOSPHORUS OXIDE CATALYST

JOHNATHAN HAR SEAN HOU

UNIVERSITI TUNKU ABDUL RAHMAN

Effect of Copper (II) towards the Physical and Chemical Properties of Vanadium Phosphorus Oxide Catalyst

Johnathan Har Sean Hou

A project report submitted in partial fulfilment of the requirements for the award of Bachelor of Engineering (Hons.) Chemical Engineering

Faculty of Engineering and Science
Universiti Tunku Abdul Rahman

May 2011

DECLARATION

I hereby declare that this project report is based on my original work except for citations and quotations which have been duly acknowledged. I also declare that it has not been previously and concurrently submitted for any other degree or award at UTAR or other institutions.

Signature : _____

Name : Johnathan Har Sean Hou_____

ID No. : 07UEB05127_____

Date : _____

APPROVAL FOR SUBMISSION

I certify that this project report entitled **"Effect of Copper (II) towards the Physical and Chemical Properties of Vanadium Phosphorus Oxide Catalyst"** was prepared by **Johnathan Har Sean Hou** has met the required standard for submission in partial fulfilment of the requirements for the award of Bachelor of Engineering (Hons.) Chemical Engineering at Universiti Tunku Abdul Rahman.

Approved by,

Signature : _____

Supervisor : Dr. Leong Loong Kong

Date : _____

Specially dedicated to
my beloved grandmother, mother and father
my friends and supervisor
and all others who supported me

ACKNOWLEDGEMENTS

I would like to thank everyone who had contributed to the successful completion of this project. I would like to express my gratitude to my research supervisor, Dr. Leong Loong Kong for his invaluable advice, guidance and his enormous patience throughout the development of the research.

In addition, I would also like to express my gratitude to my loving parent and friends who had helped and given me encouragement and strength.

Effect of Copper (II) towards the Physical and Chemical Properties of Vanadium Phosphorus Oxide Catalyst

ABSTRACT

Three VPO catalysts doped with various copper concentrations and bulk VPO catalyst were prepared via sesquihydrate method. The catalysts were characterised by XRD, BET, ICP-OES, Redox titration, SEM and EDX. It was found that the addition of trace amount of copper increases the surface area of the catalyst except 0.5 mol % copper doped catalyst. XRD, redox titration and ICP-OES analysis proved that the copper doped catalyst has higher V^{4+} compared to undoped catalyst. 0.3 mol % copper doped catalyst seems to be the best VPO catalyst in this study as further copper addition reduces the physical and chemical properties of VPO catalyst.

TABLE OF CONTENTS

LIST OF TABLES

LIST OF FIGURES

LIST OF SYMBOLS / ABBREVIATIONS

λ	wavelength, Å
VPO	vanadium phosphorus oxide
MA	maleic anhydride
FWHM	full width at half length maximum

LIST OF APPENDICES

CHAPTER 1

INTRODUCTION

1.1 Introduction

This chapter covered the basic fundamental of catalyst and catalysis, the different forms of catalysts, importance and uses of catalyst, problem statement as well as aims and objectives.

1.2 What is catalysis and catalyst

Catalyst is defined as a substance that accelerates the chemical reaction without it being consumed within the process (Chorkendorff, 2003). A catalyst can forms bond with the reacting molecules, allowing the adsorbed molecules to react between each other to form the product and then detaches itself from the catalyst. The catalyst is left unaltered so that it is available for the next reaction. Catalysis is the occurrence of using catalyst to accelerate the reaction (Chorkendorff, 2003). The diagram below shows how a catalyst functions.

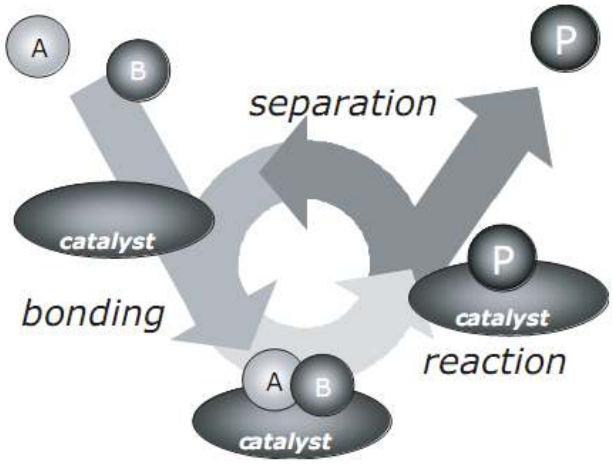

Figure 1.1: How catalyst works

The above diagram shows the catalytic reaction between reactant A and B to form product, P. It all starts with the bonding of A and B on the surface of the catalyst. Later, A and B will react between each other to form a product, P which is still bonded to the catalyst. P will then detach itself from the catalyst and the catalyst remains the same before the reaction occurs.

1.3 The forms of catalyst

Catalyst can be classified into many forms from atoms or molecules to large bulky structure such as zeolites. They also can be in liquid phase, solid phase and gas phase depending on the reaction it is required. However, all catalyst falls into three types which are biocatalyst, heterogeneous catalyst and homogeneous catalyst (Chorkendorff, 2003).

1.3.1 Biocatalyst

Biocatalysts are catalysts that exist in nature such as enzymes. An enzyme can be considered as a large protein with very shape-specific active site. The shape of the

active site is used to convert only the substrates having the same shape as the catalyst in a reaction. Thus, enzymes are highly selective and efficient catalyst.

An example of enzymes is the breakdown of alcohol to acetaldehyde inside the body by enzyme alcohol dehydrogenase. The acetaldehyde is then converted into acetate by aldehyde hydrogenase (Chorkendorff, 2003).

1.3.2 Heterogeneous catalyst

A heterogeneous catalyst occurs when the catalyst is not in the same phase as the reactant. Normally, the catalyst is in solid phase and the reactant in gas or liquid phase. Since both exist in different phase, it is easier to recover the catalyst after the reaction compared to homogeneous catalyst. Thus, heterogeneous catalyst is more often applied in the chemical industry then it counterpart due to it being more economical. For higher efficiency, solid catalyst is usually nanometer-sized particles, supported on an inert, porous structure (Chorkendorff, 2003).

An example of this type is the catalytic converter used in car exhaust. The theory behind is the catalytic oxidation of CO on the surface of platinum to form CO_2 in the presence of oxygen (Chorkendorff, 2003).

1.3.3 Homogeneous catalyst

A homogenous catalyst occurs when the catalyst is in the same phase as the reactant. Such examples are usually liquid-liquid system or gas-gas system. Seldom, solid-solid system is seen due to its low permeability between the catalyst and the reactant and low yield. It is difficult to separate the catalyst from the reactant after the reaction as both are in the same phase. Higher energy and more equipment are needed and leads to a higher production cost making it not so common in industry.

An example of this type is the catalytic carbonylation of methanol to acetic acid by rubidium complexes in solution. In this reaction, the products, reactants and catalyst are in liquid phase (Chorkendorff, 2003).

1.4 Importance and uses of catalysts

Reaction can be controlled based on four factors which are time, temperature, pressure and concentration. Among these four, raising temperature and pressure would definitely increase the rate of reaction. However, the reactor will be prone to many safety problems due to the elevated temperature and pressure. It is very difficult and expensive to build a reactor that can maintain itself at high temperature and pressure (Chorkendorff, 2003). With catalyst, the reaction temperature and pressure can be lowered to a safe level and at the same time provides reasonable rate of reaction.

Another importance of catalyst is its relation with green technology. In modern industry, the concept of green technology is very much being discussed and applied. Green technology is defined as the efficient use of raw materials, avoiding formation of waste and undesired byproducts and avoiding the use of toxic and hazardous solvent or reagent (Chorkendorff, 2003). The use of catalyst actually satisfied this theory. This is because catalyst often reduces formation of byproduct which normally encountered by using conventional method, catalyst reduces the requirement of temperature and pressure that is normally high in conventional method and finally the catalyst is normally easy to recover and reuse for the next reaction thus reducing cost and also prevent contamination of product by hazardous catalyst (though normally catalyst are metals which are not that toxic or hazardous).

1.5 Problem Statement

The application of VPO catalyst for the conversion of *n*-butane to maleic anhydride is common in the industry to obtain high conversion and selectivity. However, in practise, the VPO catalyst can only obtained *n*-butane conversion of 82% and a selectivity to form MA of 65% (BASF Petronas Chemicals Sdn. Bhd., 2010).

Many approaches had been performed to optimise the VPO catalyst for the highest *n*-butane conversion and still able to achieve high selectivity to form MA. The addition of metal dopants is one of the methods that might improve the physical and chemical properties of the VPO catalyst and is chosen in this study.

1.6 Aims and Objectives

The aim of this research is to study the effect of adding copper (II) into the bulk VPO catalyst. The objectives are as outline below:

1. To synthesis bulk VPO catalyst and copper doped VPO catalyst
2. To study the effect of adding trace amount of copper dopant towards the physical and chemical properties of VPO catalyst

CHAPTER 2

LITERATURE REVIEW

2.1 Background

Maleic Anhydride (MA) is an important intermediate used in chemical industry, more specifically, polymer industry. It is normally used in polycondensation and addition reactions. The end products of the reactions are polyester, alkyd resins, lacquers, plasticizers, copolymers and lubricants. Nearly 50% of world maleic anhydride (MA) output is used in the manufacture of unsaturated polyester resins (UPR). Chopped glass fibres are added to UPR to produce fibreglass reinforced plastics which are used in a wide range of applications such as pleasure boats, bathroom fixtures, automobiles, tanks and pipes (ICB Chemical Profile, 2010).

Global production of MA was estimated around 820,000 MT with estimated value around $ 700 million. World consumption increases at an average annual rate of 5.8% with the highest growth occurring in Asia as it is where MA is used as an intermediate for production of 1,4-butanediol (University, 2010).

The first commercial production to produce MA is by using benzene as feed and it started in 1930. Since 1985, *n*-butane was introduced to replace benzene as the feedstock and it become commercialized in 1989. The usage of *n*-butane to replace benzene in the production of MA is called ALMA process (ENEA, 1992). The basic of MA commercial success was due to the development of a highly selective catalyst, which is known as Vanadium Phosphorus Oxide (VPO).

The preparation of the VPO catalyst has been extensively studied ever since *n*-butane replaces benzene to produce MA. A numbers of parameters especially nature of the reducing agent and solvent, P/V ratio of the precursor, calcinations condition and addition of foreign materials (dopant) have been investigated. All these parameters affect the oxidation state of the Vanadium, the phase composition of the catalyst and distribution of phosphorus. Some of the parameters are discussed in section 2.3 – 2.8.

The papers studying the introduction of dopant into the VPO system is increasing recently (around 2006). However, it seems many possible dopants for VPO catalyst had been investigated in the 80's (Ballarini *et al*, 2006). Nonetheless, the study of dopant as promoter for VPO is still promising as new knowledges of the chemical-physical properties of VPO helps to discover new element suitable as a dopants or reevaluate elements which are researched last time.

2.2 Selection of VPO compared to other catalysts

There are actually three main catalysts, which are studied for alkane oxidation which includes Mg orthovanadate ($Mg_3(VO_4)_2$), Mg pyrovanadate ($Mg_2V_2O_7$) and VPO ($(VO)_2P_2O_7$. The reason VPO is chosen for conversion from *n*-butane to MA can be explained based on a table showing the typical product distribution over these three catalysts at low conversion of alkane (Kung, 1994). The table is attached as appendix A.

From the table, it is observed that using VPO catalyst for *n*-butane (C_4H_{10}) have the highest conversion, requires the lowest reaction temperature, and have an acceptable selectivity as compared with the other two catalysts. VPO catalyst is also the only catalyst compared that can form MA as a product from *n*-butane. Thus, VPO is chosen as the field of study for this project.

2.3 Different preparative routes of precursor

The morphology of crystallite structure of VPO precursor depends on the route taken to prepare it. There are currently two routes to prepare the precursor such as the aqueous route and the organic route.

In the aqueous route, V_2O_5 is reduced by a mineral agent such as hydrochloride acid (HCl) or hydrazine (N_2H_4) in water added with phosphoric acid. In the organic medium route, V_2O_5 is reduced by organic reagent such as isobutanol prior to addition of phosphoric acid. Another method in preparing the precursor is to reduce Vanadium phosphate (V^{5+}) such as $VOPO_4{\cdot}2H_2O$ with alcohol like isobutanol (Abon and Volta, 1997).

According to research, the precursors prepared by organic route give catalysts after calcinations higher specific area compared to aqueous route (Abon and Volta, 1997).

2.4 Structure of VPO phases

Vanadium exists in different phase such as V^{3+}, V^{4+} and V^{5+}. The V^{5+} phase is being related to hydrates like $VOPO_4{\cdot}H_2O$, $VOPO_4{\cdot}2H_2O$ and phosphate $VOPO_4$ (α, β, γ, and δ). The V^{4+} phase is related to hydrogenophosphates like $VOHPO_4{\cdot}0.5H_2O$, $VOHPO_4{\cdot}4H_2O$, pyrophosphate $(VO)_2P_2O_7$, metaphosphates $VO(PO_3)_2$. The V^{3+} phase is related to VPO_4 and $V(PO_3)_3$ (Abon and Volta, 1997).

2.5 Calcination parameters related to VPO catalyst

The calcination conditions are among the parameters subject to extensive studies. The calcinations parameter strongly affects the final phase composition of the catalyst and the distribution of phosphorus and vanadium and its oxidation state.

According to a research performed by a group of three in South Africa, they concluded that high gas hourly space velocities and low temperature enhances MA production (Govender *et al*, 2004). According to them, high GHSV allows the feed gas to have low residence time within the reactor, thus reducing the probability of over-oxidation of the product. Thus, it is reasonable to use high GHSV during this project to reduce the formation of undesired product.

It is reported that lower temperature favour higher selectivity as the carbon-oxide by-products are only available at high temperature although they also mentioned that *n*-butane conversion increases with temperature (Govender *et al*, 2004). Thus, a suitable temperature range with reasonable selectivity and conversion need to be determined.

2.6 VPO catalyst doped with several elements

Doping in catalysis is defined by the action of introducing small amount of foreign atom to form solid solution in the lattice of a catalyst (IUPAC, 2005-2009).

The line of authors as mentioned in parenthesis, did a research on the effect of adding several elements into the VPO system to test its characteristic, selectivity and activity. The authors used Sb, Ti, Zr, Hf, Cu and Ce as the dopants (Ieda *et al*, 2005).

The authors found out that Cu doped catalyst has higher surface area compared to a bulk catalyst. However, it has the lowest surface area if compared with other doped catalyst. The authors also proposed that surface V=O on the VPO is

responsible for the conversion of *n*-butane. It is shown that surface V=O for Cu doped catalyst is even less compared to bulk which according to the authors shows lower activity in reaction (Ieda *et al*, 2005).

From the XRD analysis of this journal, the authors observed a small shift of the (200) diffraction line for Cu doped catalyst suggesting formation of solid solution of $(VO)_2P_2O_7$ with Cu. From the DMP-TPD analysis of this journal, the authors found that addition of Cu decreases the number of Lewis acid sites and Bronsted acid sites. The authors also found the lowest propane conversion using Cu doped catalyst, far lower compared with unmodified catalyst. The selectivity also decreased for Cu doped catalyst (Ieda *et al*, 2005).

2.7 The beneficial effect of cobalt on VPO catalysts

A journal reported the effect of adding cobalt, Co into the VPO system and its characteristic and efficiency as a catalyst to convert *n*-butane into MA. Although Co is not the dopant used as the subject of this project, its discussion, method of preparation and also data interpretation are most valuable for this project.

In this journal, the authors mentioned that the best catalyst precursor is $VOHPO_4{\cdot}0.5H_2O$. They also mentioned the use of organic reductive agent such as isobutanol to convert the precursor into $(VO)_2P_2O_7$. Nonetheless, the authors said a low proportion of $VOPO_4$ phases are crucial for the catalytic reaction to function (Cornaglia *et al*, 2003).

The authors employed the organic route method in preparing their precursor which was to reflux V_2O_5 with isobutanol and benzyl alcohol for 3 h. Later, orthophosphoric acid was added into solution and further reflux for 2 h. the solid was then recovered by filtration and dried. From there, the authors used impregnation method to dope the precursor with cobalt acetate. The final step involves activating the precursor in a fixed bed microreactor (Cornaglia *et al*, 2003).

The authors employed a total of four techniques in the catalyst characterization step which are XRD, IR spectroscopy, XPS and NMR spectroscopy. XRD was used here to identify the phases existed in the VPO catalyst. The use of NMR here was to provide information of the different oxidation states of Vanadium surrounding the P atoms in $(VO)_2P_2O_7$. The use of FT-IR was to identify other phase that existed besides $VOHPO_4 \cdot 0.5H_2O$. XPS was used here to determine the elemental composition, oxidation state of elements and dispersion of one phase over another (Cornaglia *et al*, 2003).

From the discussion, the authors said Lewis acidity is important in the oxidation of *n*-butane to MA and directly involved in the activation of alkane. They found that oxidation of *n*-butane to MA is a function of both the redox properties and the acidity of the catalyst. The authors mention that promoters or dopant plays important role in controlling surface acidity of VPO. In their case, addition of Co enhances the acidity of VPO and thus increases the selectivity (Cornaglia *et al*, 2003).

Regarding the role played by presence of small amount of V^{5+} in the catalyst system, the authors reviewed a few paper and come to a conclusion. They found that industrial catalyst cannot detect the presence of V^{5+} phase and the most selective catalyst contains no V^{5+} phase (Cornaglia *et al*, 2003).

Another interesting part the authors found was that excess phosphorus not only prevents oxidation of bulk to more stable V^{5+} phases but also limits the total oxidation of surface under severe conditions (Cornaglia *et al*, 2003).

The conclusion of this journal was that Co is a nice choice of dopant to be use in the VPO system due to it increases the lewis acid site and presence of tiny V^{5+} phase thus giving it good activity, conversion and selectivity (Cornaglia *et al*, 2003).

This journal provides a brief idea on how the doped catalyst is prepared, characterised and discussed (Cornaglia *et al*, 2003).

2.8 Preparation, characterisation and catalytic properties of promoted vanadium phosphate catalyst

In this paper, some key points of VPO were reported by the authors. Their findings and conclusions are much meaningful for this project.

Firstly, VPO is considered the most suitable precursor to produce highly active and selective catalyst no matter the differences in structures and valence states. The catalyst is used in ammoxidation of various methyl aromatics (e.g. toluene) and hetero aromatics (*e.g.* methylpyrazines). Productions of those chemicals are crucial since they are widely used in many industries (*e.g.* pesticides, pharmaceutical and dyestuff) (Nagaraju *et al*, 2008).

The authors also mentioned the results of some researchers who studied the effect of a series of promoters on the VPO structure and on the density of the V=O sites. According to them, addition of slightly electronegative ions increases the number of surface V=O species and exposition of (100) plane. Also, they claimed if any one vanadium ions is replaced by a promoter ions having lower electronegative than vanadium ions, the surrounding V^{4+} ions can withdraw more electrons from neighbour oxygen atoms so that the electron density of V^{4+} increased. This act weakens the V=O bond and affects the performance of catalyst (Nagaraju *et al*, 2008).

The beneficial effect of adding promoters can be due to various reasons as quoted by the authors (Nagaraju *et al*, 2008). The major role of adding promoter is to increase the surface area of the final catalyst. Other reasons reported are:

- Increase in exposure of (020) plane when the precursor is impregnated with suitable promoter
- Increase in surface density of V=O which they considered as the active sites
- Better control of oxidation state of vanadium in the catalyst
- The promoter act electronically and enhances activation of hydrocarbon

- Formation of lattice defect which creates more active site for reaction to occur
- Form solid solutions with VPO and decrease formation of deleterious phase that generate undesired product

The authors' conclusion was that the higher performance of doped catalyst is due to the modification of VPO structure to obtain optimal vanadium oxidation state and changing the redox properties of catalyst under suitable reaction condition (Nagaraju *et al*, 2008).

CHAPTER 3

METHODOLOGY

3.1 Introduction

In this chapter, all methods adopted to conduct this study are described clearly from preparation to analysis. The following are the outlines for this chapter:

Preparation Method:

3.3 Preparation of bulk and Copper-Doped Vanadyl Hydrogen Phosphate, $VOHPO_4 \cdot 1.5H_2O$ Precursors

3.4 Preparation of bulk and Copper-Doped VPO catalysts

Analysis Method:

3.5 X-Ray Diffraction analysis

3.6 BET surface area analysis

3.7 Inductively Coupled Plasma OES

3.8 Redox titration

3.9 Scanning electron microscopy (SEM)

3.10 Energy Dispersive X-ray (EDX)

3.2 Materials and Gases Used

A list of chemicals and gases used throughout this study was as below:

1. Vanadium (V) pentoxide, V_2O_5 (MERCK)
2. ortho-phosphoric acid, *o*-H_3PO_4 (85 %) (MERCK)
3. isobutanol, $CH_3(CH_2)_3OH$ (R&M Chemicals)
4. Nitric acid, HNO_3 (R&M Chemicals)
5. Sulphuric acid, H_2SO_4 (95 % − 98 %) (Systerm)
6. Copper (II) nitrate, $Cu(NO_3)_2$ (MERCK)
7. 1 % oxygen in nitrogen (Malaysia Oxygen Berhad, MOX)
8. 99.99 % purified helium (Malaysia Oxygen Berhad, MOX)
9. Liquid Nitrogen, N_2 (Malaysia Oxygen Berhad, MOX)
10. Diphenylamine, Ph_2NH indicator
11. 0.002 M Potassium permanganate, $KMnO_4$
12. 2 M sulphuric acid, H_2SO_4
13. 0.1 M sulphuric acid, H_2SO_4
14. 0.01 M ammonium iron(II)sulphate, $(NH_4)_2Fe(SO_4)\cdot 6H_2O$

3.3 Preparation of bulk and Copper-Doped Vanadyl Hydrogen Phosphate, $VOHPO_4\cdot 1.5H_2O$ Precursors

The precursors are prepared via sesquihydrate route by the reaction of V_2O_5 (15 g from MERCK) with aqueous *ortho*-phosphoric acid, *o*-H_3PO_4 (90 ml, 85% from MERCK) in distilled water (360 ml). The mixture is refluxed in a round bottom flask placed on top of a hot plate stirrer (from Favorit) with a magnetic stirrer placed inside the flask. The reflux condition is 393 K for 24 hours. The condenser used in the reflux are equipped with a self regulated water supply system consists of a water tank and pump to prevent water shortage during the reflux.

After the reflux is finished, the flask is allowed to cool down for about two hours before the product is being harvested out from the flask. The product is a

yellow solid-liquid mixture which is identified to be $VOPO_4.2H_2O$. The $VOPO_4.2H_2O$ solid is separated from the acidic liquid via centrifuge technique. The centrifugal used is a Dynamica Velocity 14 (Figure 3.1). Here, the solid-liquid mixture is being transferred into six sample tube with equal volume between them. The centrifuge speed is 3000 rpm and the time needed is 5 min.

After centrifuging, the solid and liquid will form a distinctive layer between them and can be easily separate. The solid is salvaged and placed into an evaporating dish and placed inside an oven at 358 K for a few days to allow it to dry. The solid is periodically taken out and grind with a mortar and pestle to increase the surface area of the samples so as to allow faster drying.

When the yellowish solid is totally dried, 10 g of the solid is weigh using a analytical balances and 0.1 mol% of copper nitrate ($Cu(NO_3)_2$, from MERCK) is added using the formula attached in appendix B. The solid mixture is then added with iso-butanol (150 ml, from RandM Chemicals) into a round bottom flask and refluxed at 353 K for 24 hours.

When the reflux is finished, the product is allowed to cool down until room temperature before proceeding. The resultant product is a light blue solid-liquid mixture referred as vanadyl hydrogen phosphate sesquihydrate. The mixture is then centrifuged to obtain the solid and dried in an oven at 358 K.

The same yellowish solid ($VOPO_4$) is added with 0.3 and 0.5 mol% of copper nitrate ($Cu(NO_3)_2$, from MERCK) and follows the same procedure.

Figure 3.1: Picture of Dynamica Velocity 14

3.4 Preparation of Copper-Doped VPO catalyst

A total of four samples are prepared which are (I) bulk sample without any dopant, (II) 0.1 % Cu as dopant, (III) 0.3 % Cu as dopant and (IV) 0.5 % Cu as dopant. When all the required samples are prepared, the precursors are ready to be put into a furnace for calcinations. The furnace used is a tubular furnace. The calcinations conditions are set to 24 h, 460 °C and the gas flow is 1% oxygen/air mixture. The calcined samples are denoted as (I) bulk, (II) 0.1 % Cu, (III) 0.3 % Cu and (IV) 0.5 % Cu.

3.5 X-Ray Diffraction analysis (XRD)

3.5.1 Introduction to XRD analysis

In 1912, German physicist Max Von Laue discovered that a crystal can diffract X-rays just like a grating can diffract light of certain wavelength closes to the distance

between the ruled lines of the grating. British physicist W. H. Bragg and W. L. Bragg used Laue discovery to verify the arrangement of atoms in some crystals and develop a simple 2-D model to explain XRD. Now, XRD is commonly used to identify bulk phase and estimate particle sizes. XRD is used in catalyst characterization to identify the various phase in the catalyst. With XRD, analyst can monitor the changes of a catalyst phase as time passes.

An X-ray is produced when a chosen source is bombarded with high energy electron. An example is the use of Cu as source and produces the Cu Kα line. This occurs because the bombarding electron creates a hole in the K shell and is filled by an electron from the L shell (Moulijn, 1993).

The term XRD can be explains as the electron scattering of X-rays photons by atoms in a periodic lattice (crystalline structure). When the scattered X-rays are in phase, they will produce constructive interference. Thus, we can measure the lattice spacing, d by measuring the angle 2θ, which constructively interfering X-rays with a wavelength, λ leave the crystal using the Bragg equation (Moulijn, 1993):

$$n\lambda = 2d\sin\theta \tag{3.1}$$

where n = 1,2….

A XRD pattern is obtained using a stationary X-ray source and a movable detector. The detector scans the intensity of the diffracted radiation as a function of 2θ between the incoming and the diffracted beams.

The width of the diffraction peak can be related to the size of the particle being examined. For particle size below 100 nm, line broadening is due to the incomplete destructive interference. A formula to relate crystal size to line width is the Scherrer formula (Moulijn, 1993):

$$L = \frac{K\lambda}{\beta\cos\theta} \tag{3.2}$$

where β is the peak width, K a constant (usually taken as 1). The line broadening of the X-ray peak can be used as a rough estimation of particle size.

The disadvantage of XRD is due to its characteristic of using interference between reflecting X-rays from lattice planes. If the sample is amorphous and the size is too small, either a broad or weak diffraction lines or no diffraction can be obtained (Moulijn, 1993). This can be crucial if the catalysts contain some particles with very little size, XRD may not detect its presence. Also in rare cases, metal diffraction lines may overlap with the lines from support. Also, XRD cannot detect the surface region of the catalyst (Moulijn, 1993).

XRD can also be used to determine the crystallinity against amorphous ratio of a certain sample. The principle behind is that a sample will produce fixed intensity disregarding their phase. A sharp peak will indicates the presence of a crystalline phase and a broad peak will indicates amorphous phase. Therefore, the crystallinity ratio can be computed by calculating the area under the curve for both peaks with the formula (Moulijn, 1993):

$$crystallinity(\%) = \frac{A_C}{A_t} \tag{3.3}$$

where A_c is the area of crystalline phase and A_t is the total area under the curve.

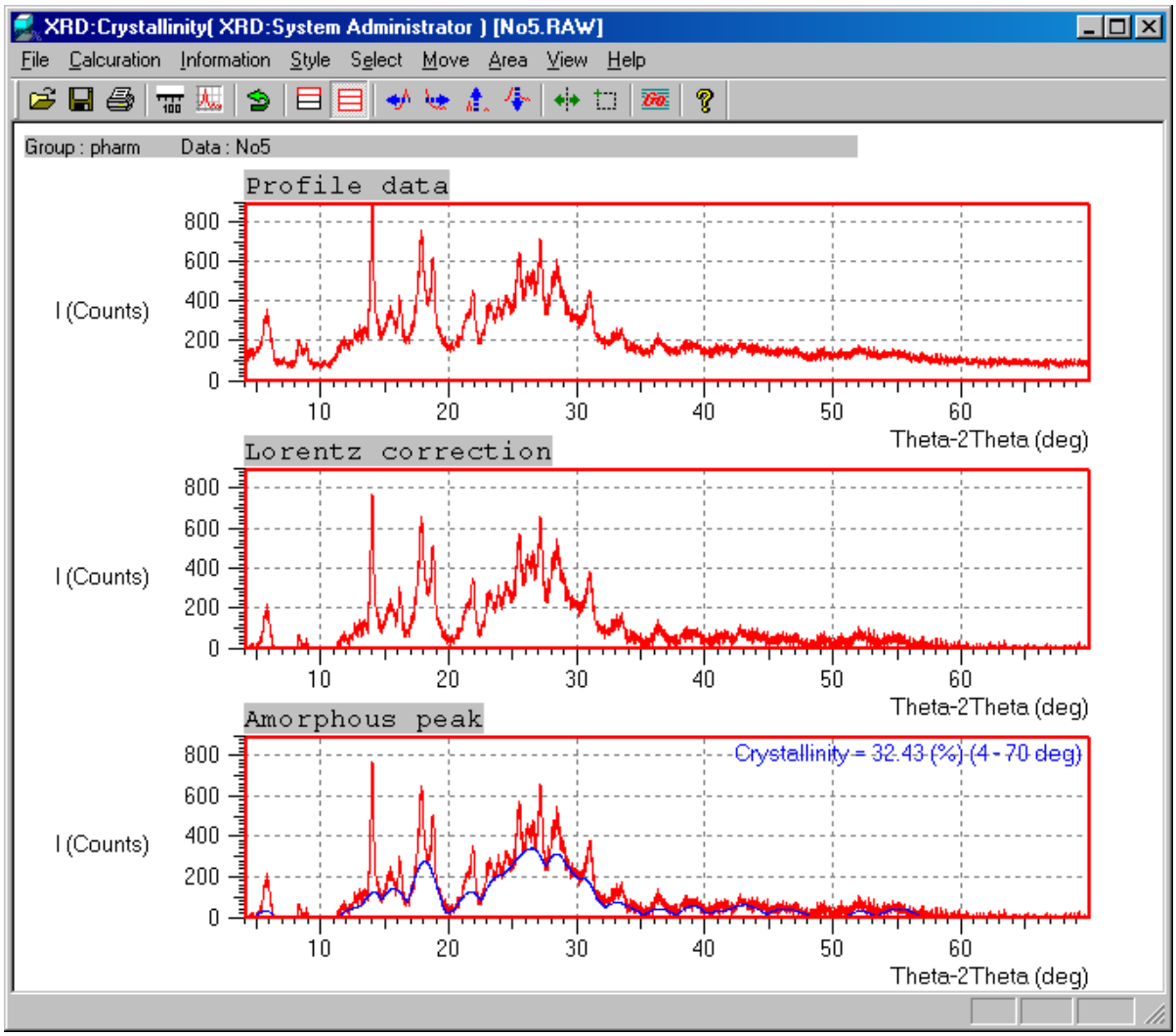

Figure 3.2: Sample data of a crystalline calculation using software

3.5.2 Procedure of XRD analysis

The XRD analysis is carried out using a Shimadzu 6000 XRD employing CuKα radiation with a scanning rate of 1.2 ° min^{-1} to generate diffraction patterns from the powder crystalline structure. The test condition is ambient temperature and the catalyst is scanned from the range of 2θ = 2°-60°. The diffractograms obtained were matched with the Joint Committee on Powder Diffraction Standards (JCPDS) PDF 1 database version 2.6 to confirm the catalysts phases.

Figure 3.3: XRD 6000

3.6 BET surface area analysis

3.6.1 Introduction to BET surface area analysis

The sorptomatic 1990 is based on the static volumetric principle to characterize solid sample by means of gas adsorption. Adsorption is defined as the concentration of gas molecules near the surface of a solid material (University of Oxford, 2010). The adsorbed gas is named adsorbate and the solid which adsorption takes place is named adsorbent. Adsorption can be classified into physical adsorption (also known as physiosorption) or chemical adsorption (chemisorption). Adsorption occurs because of the presence of an intrinsic surface energy or attractive force. For physiosorption, the force of attraction is the weak Van Der Waals force (University of Oxford, 2010). These Van der Waals forces consist of interaction between permanent dipoles, between a permanent dipole and an induced dipole, and/or between neutral atoms and molecules. This is in contrast to the stronger chemical attractions associated with chemisorption. The surface area of a solid includes both the external surface and the internal surface of the pores.

Due to the weak Van der Waals bond (less than 15 kJ/mol) associated with physiosorption, adsorption of this kind is reversible. Since gas physiosorption is non-selective, it will fill the surface step by step (or by layers) depending on the available solid surface and the relative gas pressure. By filling up the first layer, we can measure the surface area of the material since the amount of gas adsorbed when the mono-layer is saturated is proportional to the entire surface area of the sample. The adsorption/desorption analysis is called an adsorption isotherm (Moulijn, 1993). For different method of gas/solid interactions, six IUPAC standard adsorption isotherms are created (IUPAC, 1985):

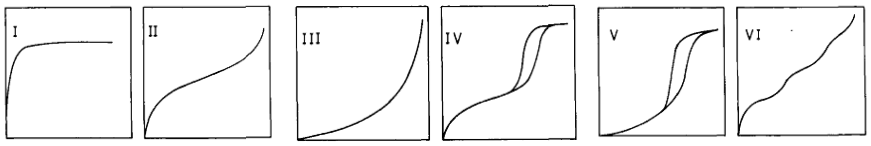

The monolayer capacity of a solid is defined as the amount of adsorbate that can be accommodated in a completely filled single molecule layer on the surface of one gram of solid. Most surface area determinations are done using nitrogen molecules as yardstick and nitrogen isotherm being measured at its boiling point of 77.4 K (Moulijn, 1993).

Brunauer, Emmett and Teller introduced an adsorption model that allows for adsorption in multilayer in 1938. The concept of BET theory is actually a variants of Langmuir isotherm (monolayer adsorption) modified to fit multilayer adsorption (Moulijn, 1993). Thus the assumptions made in deriving Langmuir isotherm is applied which are

- All adsorption sites are equally active
- Surface of adsorbent is flat
- No interaction between each adsorption layer and between the adsorbed molecules itself
- Gas molecules physically adsorbed on a solid in layers infinitely
- Adsorbed molecules are localized (immobile)

The disadvantage of BET theory is that it only holds for isotherm type II and IV. Also, BET only works in a BET region where the range of partial pressure is from 0.05 to around 0.3 (Moulijn, 1993).

3.6.2 Procedure of BET surface area analysis

The total surface areas of catalysts are measured by using nitrogen adsorption at 77 K. This is done by ThermoFinnigan Sorptomatic 1990. The complete procedure includes a pre-treatment step to remove any contaminant from the catalyst such as unwanted gases prior to the analysis. The pre-treatment condition are a gas flow of nitrogen at 20 cm^3/min, 1 bar, 473 K and a holding time of 30 min before cooling back to ambient temperature. In the analysis step, pure nitrogen gas was injected to fill the catalyst pores and later it undergoes desorption. The surface area is calculated based on the amount of nitrogen being adsorbed and desorbed. A blank test is also performed using helium gas rather than nitrogen gas to reduce the error in the actual surface area value. The surface area calculation is performed by the software automatically after all requires information is inputted.

Figure 3.4: Sorptomatic 1990

3.7 Inductively Coupled Plasma OES

3.7.1 Introduction to ICP-OES analysis

Atomic emission spectroscopy (OES) is the study of the radiation emitted by excited atoms and monoatomic ions. When an excited atom and ions relax to ground state, light is emitted producing line spectra in the UV-Vis regions (Robinson, 2005).

OES can be used for the qualitative identification of an element presents in the sample or for quantitavie analysis of the elements at low concentration (ppb) (Robinson, 2005). Since long ago, the excitation source for OES is always been flames or an electrical discharge. Now, a new source, which is the inductively coupled plasma (ICP) has been introduced. The major differences between the different type of OES lies in its excitation source and the energy delivered to the ions or atoms. ICP is a high energy source that can excite most elements (metal or nonmetal) and produce very line-rich spectra (Robinson, 2005).

The advantage is that many elements emit multiple wavelengths simultaneously and thus we have more choice of wavelengths for each element and can measure multiple elements simultaneously. Another advantage is the high temperature of plasma reduces many chemical interference found in flame source OES (less matrix effect) (Robinson, 2005). The disadvantage is that as the number of emission wavelength increases, the interference increases and overlapping of line is possible. Plasma is a type of matter containing large amount of electrons, ions, radicals and neutral species. It is electrically conductive and affected by magnetic field. Commercial ICP uses argon ICP as plasma source. The temperature of plasma ranges from 6500 to 10000 K, almost any elements are atomized and excited to multiple levels resulting in line-rich spectra (Robinson, 2005).

The light emitted by the OES follows the Planck-Einstein equation $E = hc/\lambda$, where h is Planck's constant, c is velocity of light and λ is wavelength. Since h and c is a constant, the energy released can be said to be exclusive with the element unique wavelength. Also, the intensity of energy emitted at a chosen wavelength is proportional to the amount (concentration) of that element in the sample being

analysed. Thus, by determining the wavelengths emitted and its intensity, we can identify the elements present in the sample using fingerprint matching with a reference standard (Robinson, 2005).

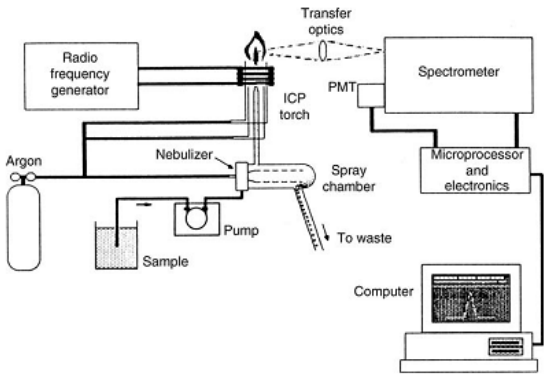

Figure 3.5: ICP-OES diagram

3.7.2 Procedure of ICP-OES analysis

The procedure of ICP-OES begins with the preparation of standard and stock solutions for Vanadium, Phosphorus and Copper. A blank solution is also prepared as it is required by the Spectrometer. After the preparation of standard and stock solutions, the test samples which are bulk sample, 0.1 % Cu, 0.3 % Cu and 0.5 % Cu are dissolved using 8M of nitric acid and topped up using deionised water to 250 ml. Lastly, all solutions (test samples, standard solutions and stock solution) are transferred into test tubes to be ready for the ICP-OES analysis.

The bulk and doped catalysts chemical composition are determined by a Perkin-Elmer Emission Spectrometer Model Plasma 1000. The sampling is performed by an automated sampler programmed by the software and the final results are shown as a text file.

Figure 3.6: ICP-OES instrument

3.8 Redox titration

The acidity characteristics of the solid samples are measure using a potentiometric titration method termed Niwa and Murakami Method (Niwa and Murakami, 1982). Miki Niwa and Yuichi Murakami researched the reaction mechanism of ammoxidation of toluene on V_2O_5 / Al_2O_3 catalyst. In their paper, they proposed a method of redox titration to calculate the average oxidation state of vanadium.

A known mass of sample, suspended in sulphuric acid is stirred for 3 h and then titrate with a solution of 0.01 N potassium permanganate solutions. This is to oxidise V^{3+} and V^{4+} in the solution to V^{5+}. The titration ends when the colour of solution changes from greenish blue to pink. Then, the same solution is treated with 0.01 N of ammonium iron (II) sulphate solution. This is to reduce the V^{5+} in the solution to V^{4+}. The titration ends when the purple colour of solution changes to colourless.

Another fresh 25 ml of the original sample/acid solution is titrated with 0.01 N of ammonium iron (II) sulphate solution. This is used to determine the V^{5+} in the

original solution. The titration ends when the purple solution changes to greenish blue.

The equation used is as follows:

$$AV = \frac{5V^{5+} + 4V^{4+} + 3V^{3+}}{(V^{5+} + V^{4+} + V^{3+})} \tag{3.4}$$

where V^{3+}, V^{4+} and V^{5+} are concentration of vanadium at different oxidation state. To calculate the values above, other equations are needed:

$$V^{3+} = 20(0.01)V_1 - 20(0.01)V_2 + 20(0.01)V_3 \tag{3.5}$$

$$V^{4+} = 40(0.01)V_2 - 40(0.01)V_3 - 20(0.01)V_1 \tag{3.6}$$

$$V^{5+} = 20(0.01)V_3 \tag{3.7}$$

where

V_1 = volume of potassium permanganate used

V_2 and V_3 = volume of ammonium iron (II) sulphate used

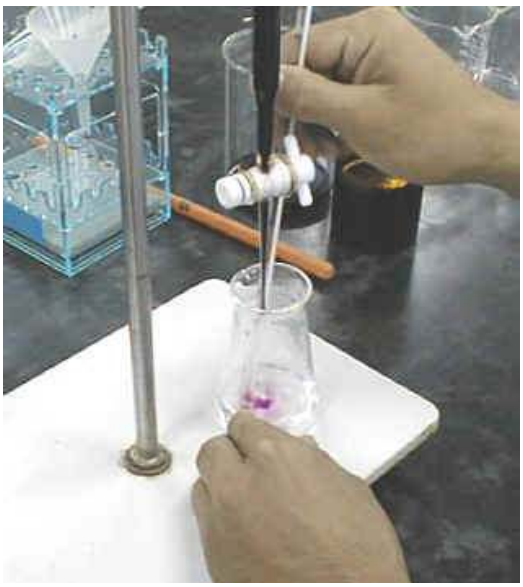

Figure 3.7: Sample of redox titration

3.9 Scanning electron microscopy (SEM)

3.9.1 Introduction to SEM analysis

SEM is basically a microscope that utilises electrons instead of light to form the image (Radiological and Environmental Management, 2010). The development of SEM can be traced back to early 1950 and its usage is broad. SEM is widely used in catalysis, medical, bio-engineering and physical sciences. SEM enables researchers to examine their samples much better due to its characteristic that allows higher resolution at high magnification (about 10,000x to 100,000x).

SEM main components include electron gun, magnetic lens, scanning coils, electron detector, computer screen, stage and specimen holder. Among all the components, the electron gun is the most important as this is where the electron used is produced. The electron beam follows a vertical path through the microscope which is held in vacuum to prevent any collision with air particles. The beam travels through an electromagnetic field and lens that focus the beam towards the specimen. Once the beam hits the specimen, electrons and x-rays are knocked out from the sample. The detector will then collects these released electrons and x-rays, converting them into signal that is shown in a computer screen (Radiological and Environmental Management, 2010).

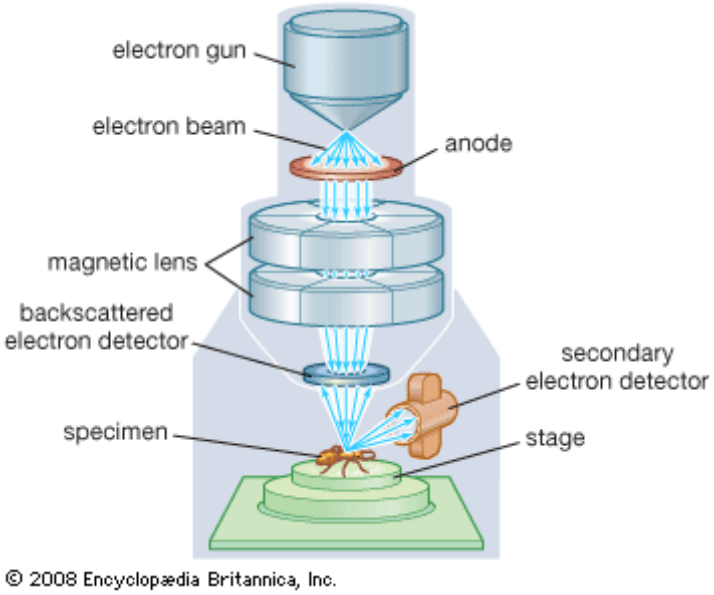

Figure 3.8: SEM schematic

Figure 3.9: Picture of Hitachi S3400N

SEM requires that the specimen being analysed to be conductive (Radiological and Environmental Management, 2010). Thus, if the sample being used is an inorganic, a special step called coating needs to be done. Coating means to

cover the specimen with a thin layer of conductive material such as platinum or gold. The device used in coating is called a sputter coater (Radiological and Environmental Management, 2010). Special care is made during the coating process to ensure that the specimen is fully covered by the conductive material as to prevent any unwanted noise generated during the SEM analysis.

Figure 3.10: Picture of Sputter coater

3.10 Energy Dispersive X-ray Spectroscopy (EDX)

The EDX is basically an add-on for the SEM and it is not functional alone. It is a chemical microanalysis technique used to identify the elemental composition of a material (Cranfield University, 2007). This technique as compared to wet chemical analysis is much better as it provides (Samuel Roberts Noble Electron Microscopy Laboratory, 2010):

1. Non destructive analysis
2. Good sensitivity of > 0.1% for elements heavier than carbon
3. Require samples as little as micrograms
4. Able to analyse samples as small as 20 to 200 nm

Figure 3.11: Picture of EDX analyser

However, EDX analysis is less accurate compared to wet chemical analysis due to the fact that only a chosen particle is being analysed in the EDX. Thus, the result will not show the general element composition of the material. This is particularly true if one is using the EDX to confirm the availability of a certain element inside the sample. If the element percentage within the sample is very low (about 0.05-0.1 mol %), there is a possibility that the element cannot be detected at all.

The principle of EDX is to detect and collect x-rays produced by a sample being bombarded by electron beam. When a particle is being bombarded by electron beam, it is excited to a higher energy level and x-rays are produced. The energy of the x-rays is unique to the element that produced them (Cranfield University, 2007). EDX then collect all the x-rays being emitted by the particles, converting it to electrical signal and showing it as a graph of energy versus counts in the computer. From there, the software will compare the result with an element database to identify the peaks.

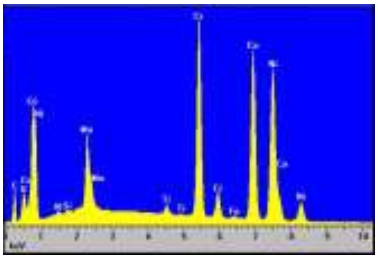

Figure 3.12: Sample of EDX spectrum from website

3.10.1 Procedure to SEM and EDX analysis

The surface structure and the morphology of the bulk and doped VPO catalyst are analysed by using a Hitachi S-2400N SEM. Prior to the analysis step, small amount of the test samples are placed on the multi sample holder and labelled accordingly. The sample holder are then placed in the sputter coater and coated with a layer of platinum. After the coating process, the sample holder is placed into the SEM and the environment inside the SEM is vacuumed. After the vacuum process, the samples are ready for SEM and EDX analysis. The test condition is 15 kV for SEM analysis and two pictures are taken for each sample with different magnification.

EDX analysis is run in conjunction with SEM analysis. The analyser used is EDAX EDS analyser. The purpose is to double confirm the existence of Copper in the VPO catalyst. The EDX software automatically measures the amount of count for elements within a chosen part of VPO particles and the result is shown as a text file.

CHAPTER 4

RESULTS AND DISCUSSION

4.1 X-ray diffraction (XRD)

The XRD patterns of the addition of copper into the VPO catalyst are shown in Figure 4.1 and the XRD patterns for precursor are shown in Figure 4.2.

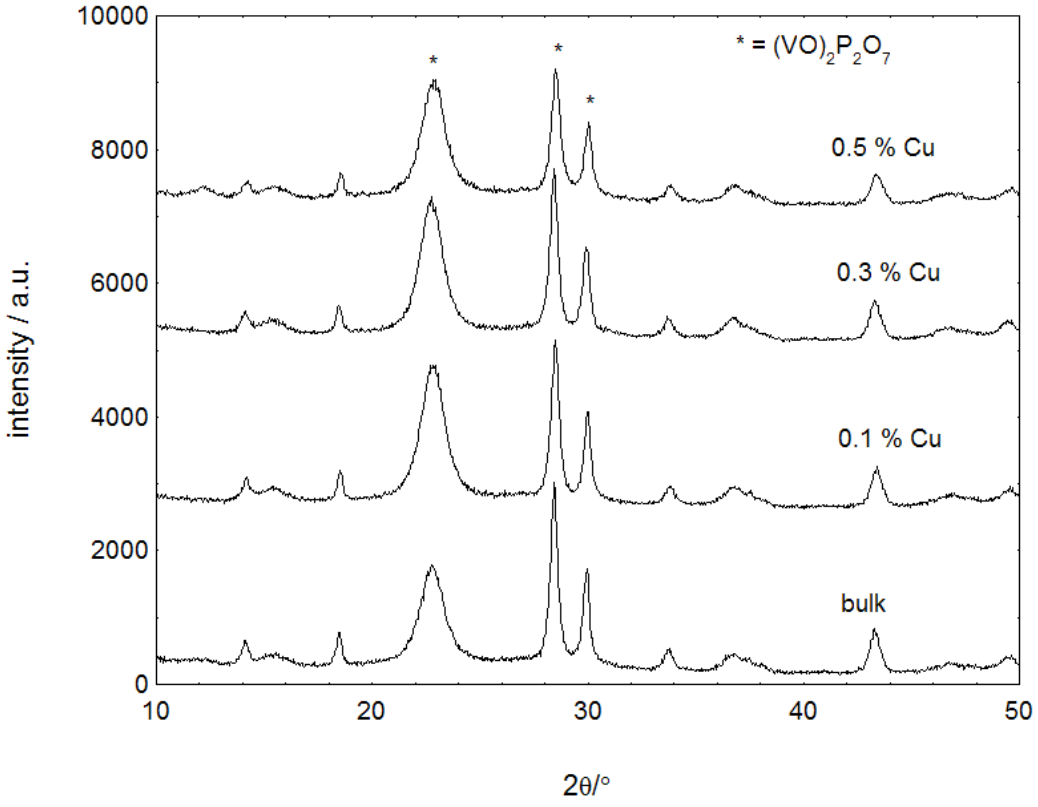

Figure 4.1: XRD patterns of undoped and Cu-doped VPO catalysts

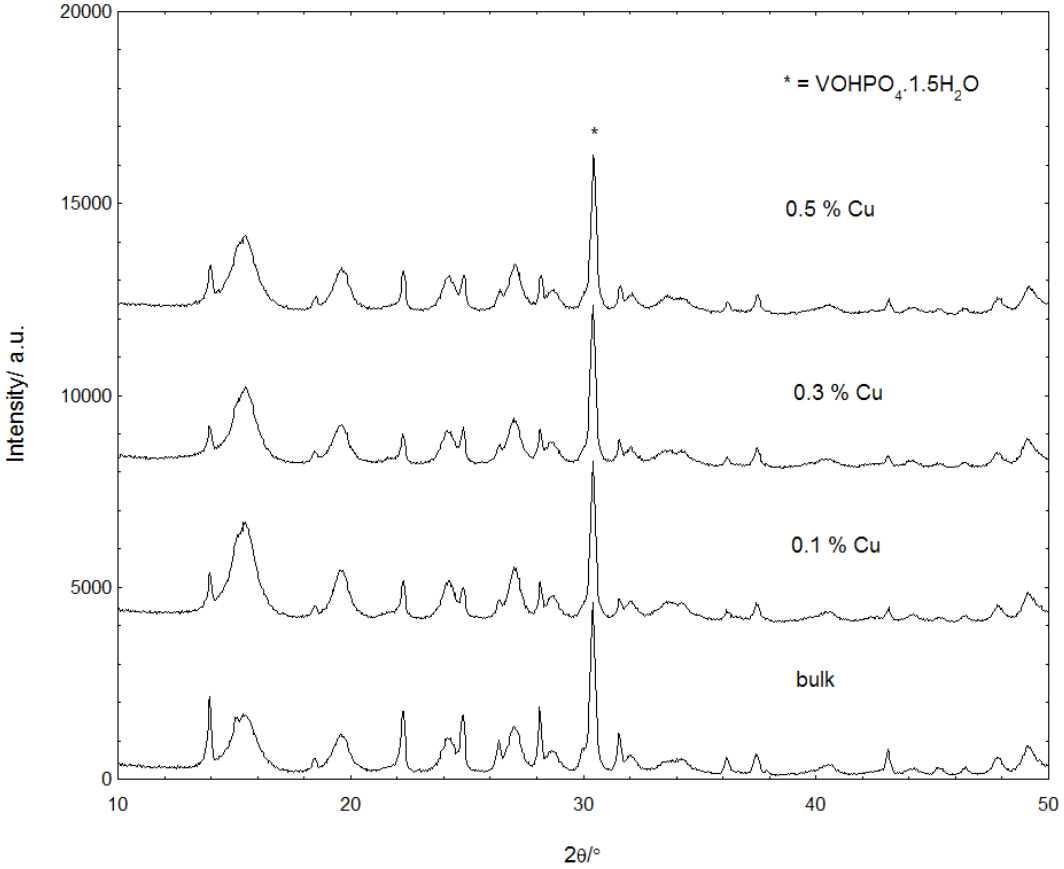

Figure 4.2: XRD patterns of undoped and Cu-doped VPO precursors

The table below shows the estimated crystallite size for the three main peaks in the $(VO)_2P_2O_7$ phase. The full calculation and raw data are attached in the appendix section.

Table 4-1: Crystallite size estimation for $(VO)_2P_2O_7$ phase

Catalyst	(020) Å	(204) Å	(221) Å
Bulk	59.25	129.18	129.80
0.1 % Cu	61.11	127.26	130.36
0.3 % Cu	61.48	120.49	121.73
0.5 % Cu	60.11	114.03	116.49

The table below shows the crystallinity against amorphous ratio for all the samples. The results are computed using the software provided with XRD 6000 and no manual calculation is involved.

Table 4-2: Crystallinity ratio (%)

Catalyst	Ratio %
Bulk	29.45
0.1 % Cu	32.53
0.3 % Cu	31.69
0.5 % Cu	28.24

From Figure 1, it is observed that the XRD patterns for all samples show the characteristic reflection of $(VO)_2P_2O_7$ phase with main peaks at $2\theta = 22.7°$, 28.2° and 29.8°, corresponding to (0 2 0), (2 0 4) and (2 2 1) planes, respectively (Goh and Taufiq-Yap, 2007). As seen from table 4-1, the (0 2 0) plane seems to increase from 59.25 Å in bulk VPO to 61.48 Å in 0.3 % Cu whereas the (2 0 4) plane shows a decrease from 129.18 Å in bulk VPO to 120.49 Å in 0.3 % Cu.

The peak intensity shows an increasing trend at 0.1 % Cu concentration to 0.3 % Cu and decreases at 0.5 % Cu concentration. Since $(VO)_2P_2O_7$ phase is a major V^{4+} phase as indicated by the literature review in Section 2.7, this means that the addition of low quantity of copper promotes the formation of V^{4+} phase in the catalysts where the optimal value is 0.3 % Cu concentration. Any higher Cu concentration will start to lower the formation of V^{4+} phase as shown by the 0.5 % Cu. This result is in agreement with the redox titration result which showed the same trend. The V^{4+} of the catalyst is always being referred as the active site of the VPO catalyst and the V^{5+} controls the selectivity of C_4 oxidation to MA. Thus, a deduction can be made from the XRD result that all the copper doped catalysts have higher activity than the bulk catalyst.

In Figure 2, the XRD patterns for all samples show the characteristic reflection of $VOHPO_4 \cdot 1.5H_2O$ phase with main peaks at 2θ = 30.4° referring to another paper (Taufiq-Yap *et al*, 2004). This observation proves that our precursors are consist mainly of the $VOHPO_4 \cdot 1.5H_2O$ phase suitable to be converted to $(VO)_2P_2O_7$ phase after calcination. The checking of precursors is very important as it may save many troubles to identify the problem if there is an unacceptable result during physical and chemical analysis. One can spend a lot of time troubleshooting the catalyst but not aware that the problem lies at the early stage within the precursor steps.

Crystallite sizes can be estimated based on X-ray peaks broadening by using the Debye-Scherrer equation (Leong *et al*, 2010):

$$t = \frac{0.89\lambda}{FWHM \cos\theta} \tag{4.1}$$

where t is the crystallite size for the desired peak, λ is the X-ray wave length for Cu Kα, FWHM is the full width half length of the desired peak and θ is the diffraction angle for that peak.

From Table 4.1, it is observed that the crystallite size of the (0 2 0) phase for doped catalyst is larger compared to the undoped catalyst. For both (2 0 4) and (2 2 1) phase, the crystallite size is decreasing with increasing copper concentratation. Although there is a slight increase in crystallite size for 0.1 % Cu in (2 2 1) phase, the size increase is very small compared to bulk and can be assumed to be the same, thus showing a general decreasing trend for that particular plane.

An observation of the XRD profiles for catalyst is that the diffraction line for 0.5 % Cu doped catalyst is slightly shifted as compared to others. This is shown in the 2θ value between all four catalysts referred at appendix C. The 2θ value for (2 0 plane changed from 28.4° (JCPDS file No. 34-1381) to 28.5° for 0.5 % Cu. By referring to literature review in Section 2.9, this phenomena can be identified as the formation of solid solution between $(VO)_2P_2O_7$ and Cu. The formation of solid solution is thought of capable in decreasing the formation of deleterious phase in the

catalyst and produces less undesired product when use in the *n*-butane reaction as reported by Section 2.11. However, this statement cannot be proven in this study since the catalytic experiment is not being performed.

Another finding from the XRD profiles of catalyst is that the diffraction data for copper cannot be detected. However, the existent of copper within the samples can be proved by using ICP analysis, EDAX analysis and even by referring to the XRD profiles of precursor using the database software provided. This suggests that copper is either being incorporated into the lattice of $(VO)_2P_2O_7$ similar to the case of iron promoter (Taufiq-Yap *et al*, 2005) or the amount of copper is too low to be detected by the XRD (Nagaraju *et al*, 2008).

The results in Table 4.2 are shown as a ratio percentage. This means that for bulk sample with 29.45 %, the interpretation is a mixture of crystalline-amorphous phase with 29.45 % crystalline phase and the remaining 70.55 % amorphous phase.

The addition of 0.1, 0.3 and 0.5 mol % copper shows a decreasing trend with 0.5 mol % copper actually reduces the crystallinity percentage below than that of bulk sample. However, the percentage changes of adding copper into the system is very small ranging from 1.21 % to 3.08 %. Based on this interpretation, it can be seen that the addition of copper into the VPO catalyst didn't much affects the crystalline phase of the catalyst.

4.2 BET surface area analysis

The table below shows the result obtained from ThermoFinnigan Sorptomatic 1990. No manual calculation is involved as the software automates every calculation and only shows the result.

Table 4-3: BET surface area analysis

Catalyst	Surface area m^2g^{-1}
Bulk	12.95
0.1 % Cu	13.78
0.3 % Cu	16.66
0.5 % Cu	10.17

The surface area of the unmodified VPO catalyst is found to be 12.9522 m^2g^{-1}. This value is actually within the range if compared to the undoped VPO value published in various papers. By comparing a few papers, it is found that unmodified VPO is generally between the ranges of 7.8 to 35.8 m^2g^{-1} (Taufiq-Yap *et al*, 2006; Taufiq-Yap, 2006; Nagaraju *et al*, 2008).

The reason of this huge range of surface area is due to the differences in preparation variables. Variables such as calcinations temperature, calcinations gas used, precursor route, reflux duration and temperature all affects the surface area.

From Table 4.3, it is shown that the trend is increasing from 0.1 % Cu to 0.3 % Cu. One explanation is that the addition of copper at low quantity acted as a good structural promoter where it enters and modified the basal (1 0 0) plane structure of VPO catalyst (Leong *et al*, 2010). The (1 0 0) plane is considered to be the main factor that cause high surface area in VPO catalyst as reported in other source (Taufiq-Yap *et al*, 2006). However, there is a reduction of surface area experience in 0.5 % Cu. A suggestion is that the relatively bigger size of copper atom as compared to the smaller size VPO causes the internal pores to be covered up by the copper atom leading to lesser surface area.

Surface area plays an important role in catalysis. Higher surface area means more active site for the reactant to attach and form the product. Therefore, a hypothesis can be made that the activity of copper doped catalyst will be higher than undoped catalyst with 0.3 % Cu being the optimal amount of copper need to be added into the catalyst for better activity.

4.3 Inductively Coupled Plasma OES

The table below shows the result obtained from Perkin-Elmer Emission Spectrometer Model Plasma 1000. The data obtained is reported in mg/L which is later converted into mol and the ratio between P and V as well as Cu and V is calculated. The complete calculation is attached in appendix.

Table 4-4: ICP OES analysis

Catalyst	P mol	V mol	Cu mol	P/V	Cu/V
Bulk	0.00077616	0.000604811	0	1.28	0
0.1 % Cu	0.000713848	0.000530805	6.79822E-06	1.34	0.013
0.3 % Cu	0.000633132	0.000514904	7.34901E-06	1.23	0.014
0.5 % Cu	0.000633455	0.000474858	8.08863E-06	1.33	0.017

By referring to Table 4.4, it is found that the range of P/V ratio for bulk catalyst and copper doped catalyst is between 1.23 to 1.34. The data also shows that doped catalyst can provide more phosphorus content due to an increase in P/V ratio between undoped and doped catalyst. The same phenomena are also reported by other authors where most found that doped catalyst normally produces higher P/V ratio (Taufiq-Yap *et al*, 2006; Leong *et al*, 2010). Furthermore, ICP OES analysis confirmed the presence of copper within the catalyst where its presence is not detected by XRD. This supported the reason where copper may incorporate into the lattice of the catalyst structure.

The range of P/V ratio obtained in this experiment is quite acceptable as according to literature the optimal value for P/V ratio is 1.5 to 3.0 (Vadim and Moises, 2005). The excess amount of phosphorus prevents the oxidation of V^{4+} to V^{5+} such as mentioned in Section 2.10. By maintaining the V^{4+} phase while limiting the V^{5+} phase, catalyst with high activity and good selectivity can be obtained. Based

on the facts above, an assumption can be made that copper doped catalyst can give slightly better activity with good selectivity compared to undoped catalyst.

The 0.3 % Cu shows a value below the undoped catalyst contradicting the overall result. By referring to the data, the correct value of 0.3 % Cu should be around 1.33-1.34; this is most likely due to accumulated error. Accumulated error here means that there are many small minor errors that can or cannot be avoided during the ICP OES analysis which after accumulated makes a huge error. Some of the potential errors are preparation of the sample solutions, non-homogeneous samples and instrument problem.

Basically the preparation of element solutions should be correct since the instrument will need to plot a standard calibration curve before analysis is allowed to proceed. The only preparation problem that can occur is therefore within the sample solution. The catalyst may not be completely dissolved within the acid solution and thus affects the accuracy of the result.

The samples may also be non-homogeneous. This is due to the facts that this experiment is conducted using low amount of copper dopant. Because the dopant amount is so small and only 0.1 g of sample is added into acid to make the sample solution, it is possible that there is very less elements presence in the sample solution or the detected result differences can be very small.

The Perkin-Elmer Emission Spectrometer Model Plasma 1000 is also a possible error contributor. This instrument is a department property where any students can use it for their study. The problem is that contaminant can occur where the previous user solution affects the current user solution. This could occur if the previous user didn’t clean the instrument as per instruction or simply because their solution is very resilient. Other possible reasons for instrument error are like wrong setting by previous user, plasma not working correctly and the detector is out of calibration.

4.4 Redox titration

The table below shows the processed redox titration result. All raw data and full calculation is attached as appendix.

Table 4-5: Redox titration results

Catalyst	V_{avg}	V^{4+} %	V^{5+} %
Bulk	4.1700	83.00	17.00
0.1 % Cu	4.1593	84.07	15.93
0.3 % Cu	4.1488	85.12	14.88
0.5 % Cu	4.2522	74.78	25.22

The redox titration calculation proposed by Niwa and Murakami to calculate the average oxidation state is a direct indication of V^{5+} percentage. Thus, an undoped bulk sample with 4.17 average oxidation numbers means it has 17.00 % of V^{5+} and 83.00 % V^{4+} oppositely.

As mentioned before good catalysts need to have high amount of V^{4+} and small amount of V^{4+} in order to obtain high activity and good selectivity. Thus, a deduction can be made where optimal addition of copper into the catalyst can promote the formation of V^{4+} phase, gives better activity to the catalyst compared to undoped catalyst. Based on data obtained in Table 4.5, the highest V^{4+} percentage is achieved in 0.3 % Cu. Thus, 0.3 % Cu is the optimum amount needs to be added into the VPO catalyst for highest activity and good selectivity.

From the result obtained, it can be seen that the V^{5+} percentage is actually quite big from 14.88 % to 25.22 %. However, referring back to the XRD patterns, peaks corresponding to V^{5+} is very hardly noticeable and only shows up in the software identification. This shows that XRD is not so sensitive in detecting small amount of V^{5+} phase. The same finding is reported in a paper mentioning that 20 % of V^{5+} may exist without a clear peak shown in the XRD pattern (Taufiq-Yap and Saw, 2008).

4.5 SEM - EDAX

4.5.1 SEM

The followings are the SEM micrographs of bulk VPO, 0.1 % Cu, 0.3 % Cu and 0.5 % Cu.

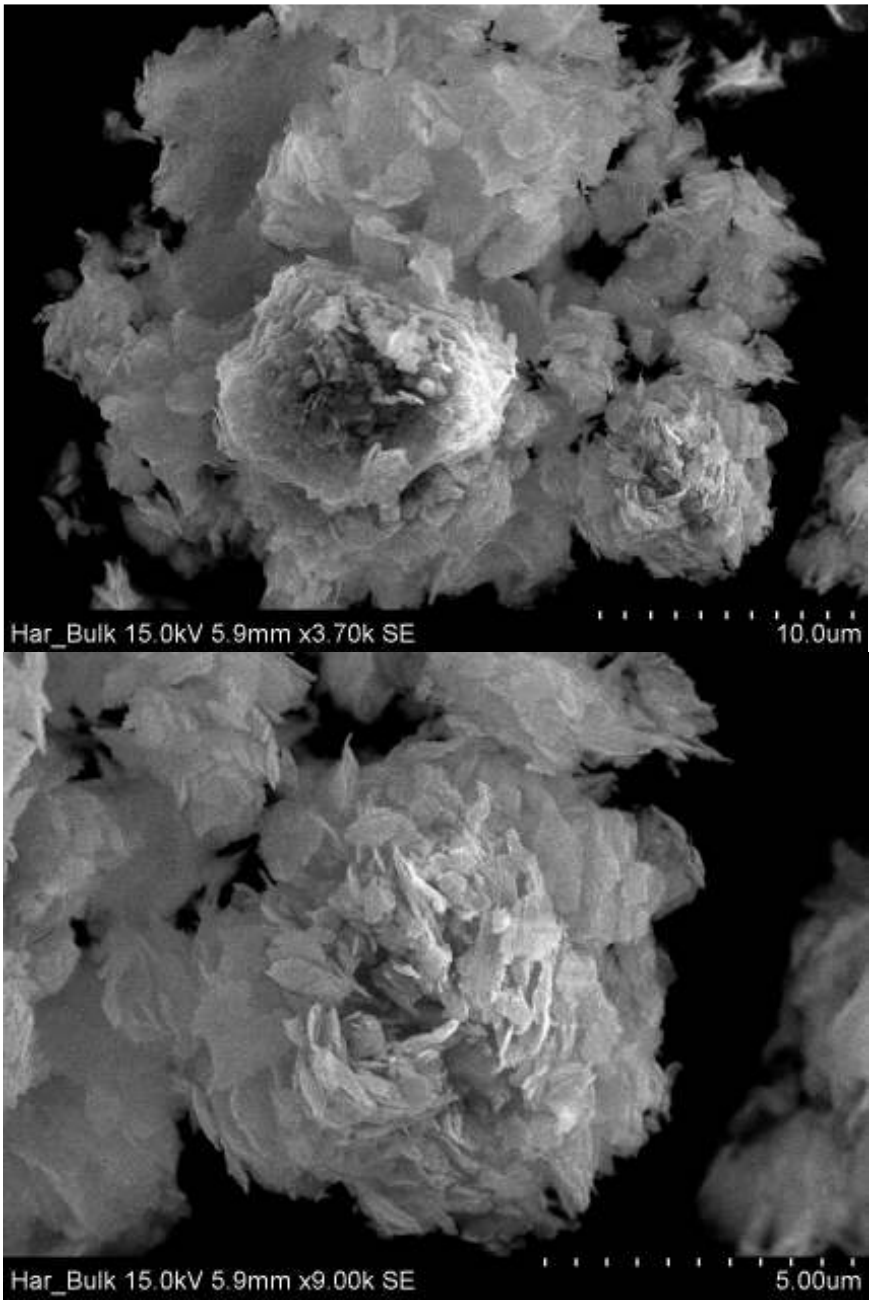

Figure 4.3: SEM picture of bulk VPO catalyst with different magnification

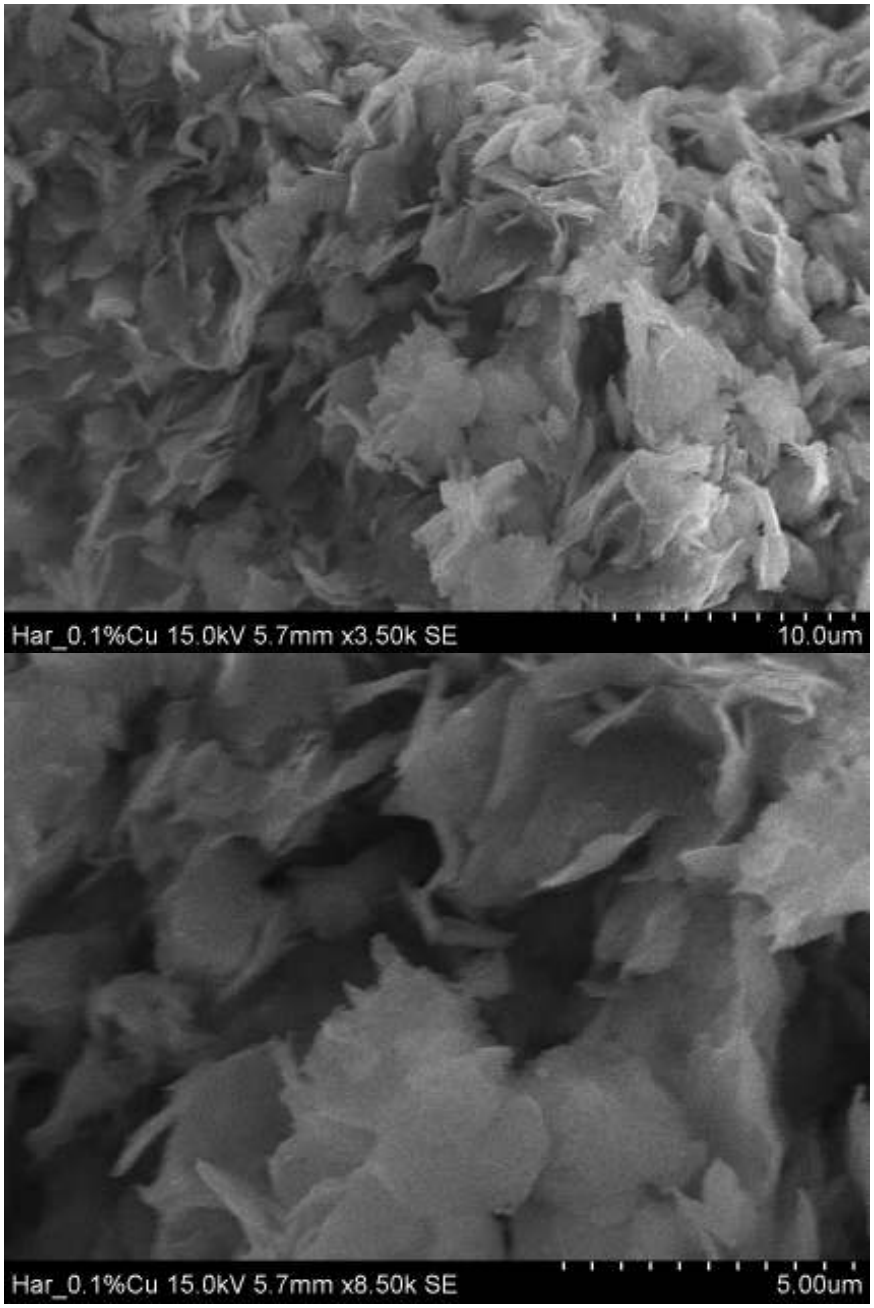

Figure 4.4: SEM picture of 0.1 % Cu doped VPO catalyst with different magnification

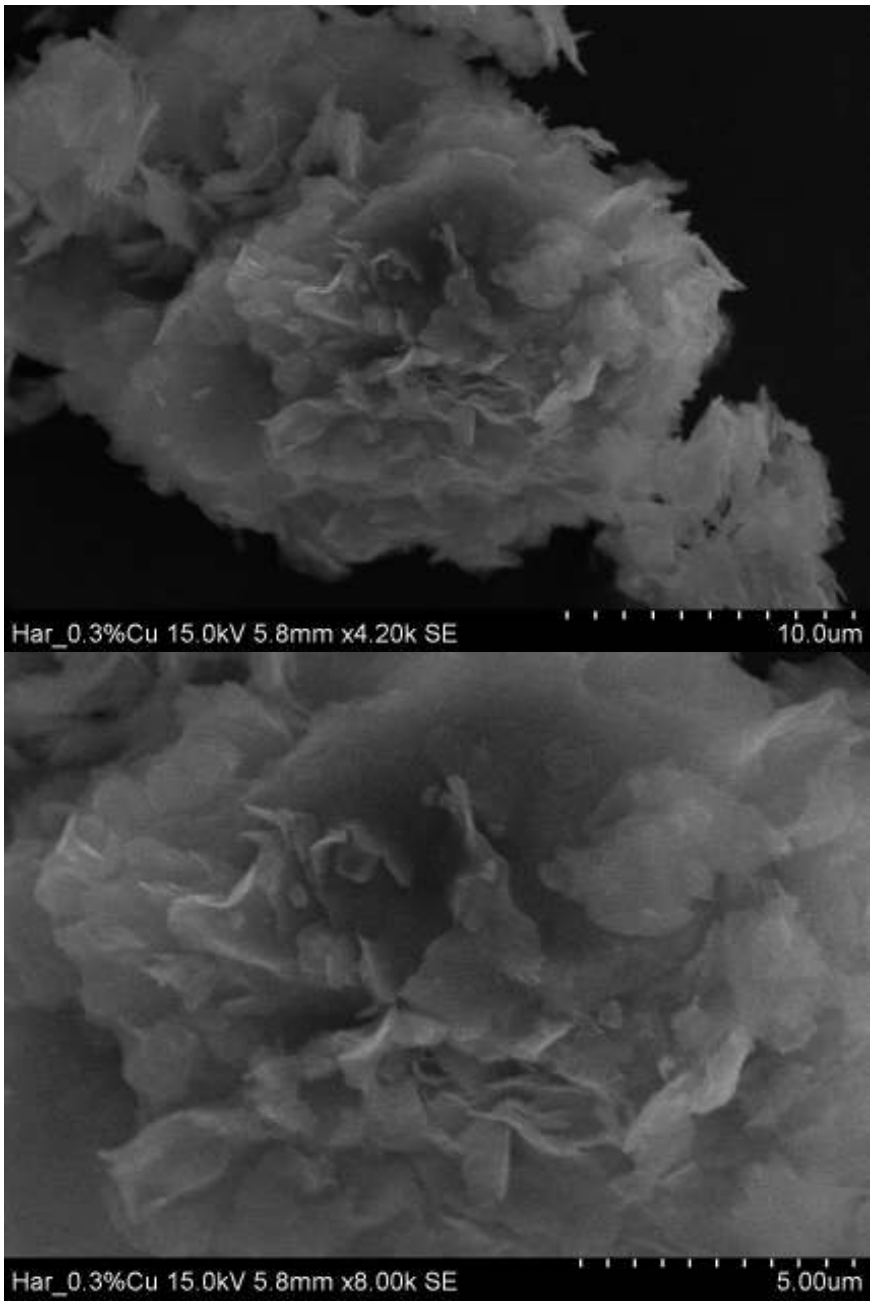

Figure 4.5: SEM picture of 0.3 % Cu doped VPO catalyst with different magnification

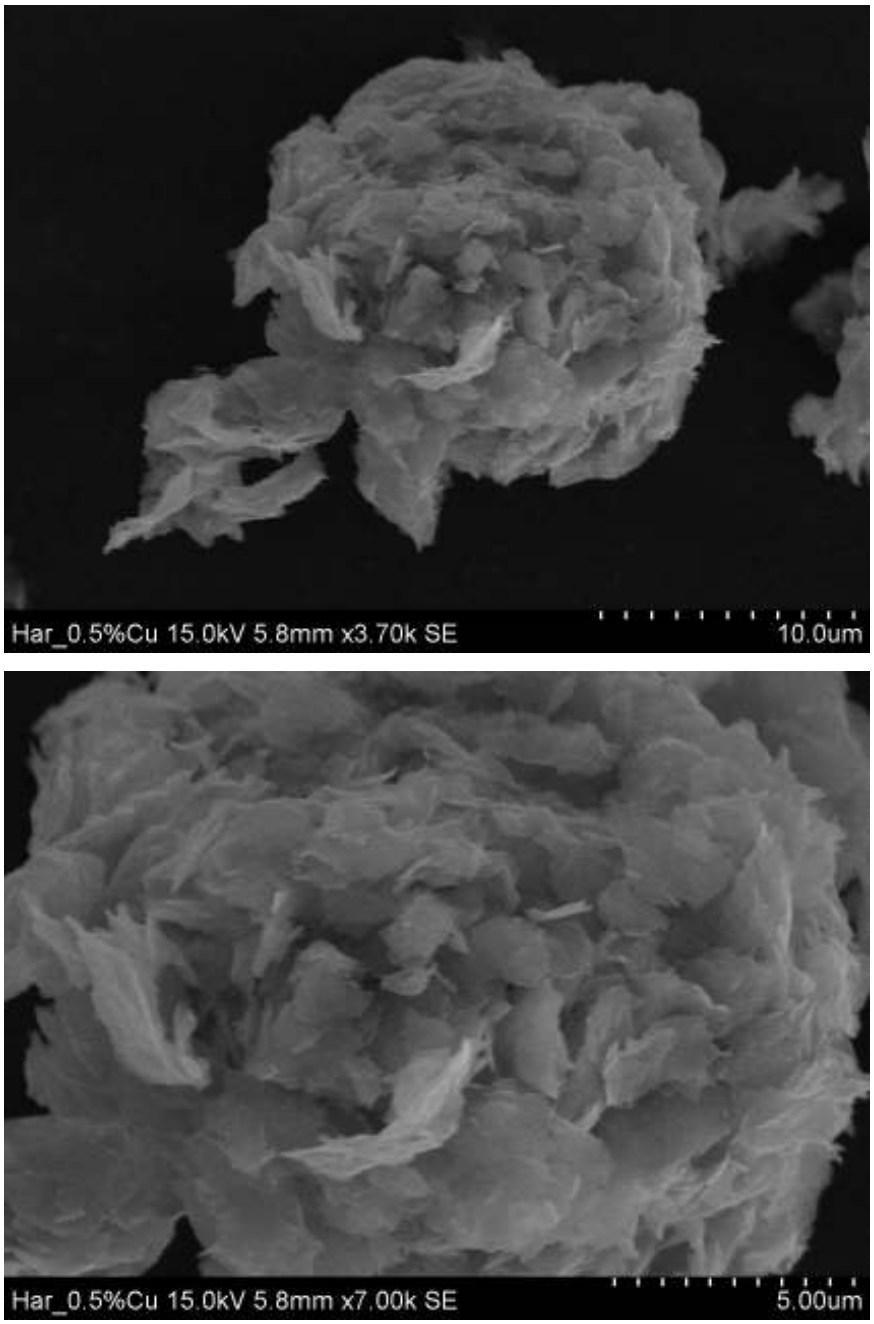

Figure 4.6: SEM picture of 0.5 % Cu doped VPO catalyst with different magnification

The SEM micrograph of the VPO catalyst composed of plate-like crystallite cluster. Referring other literatures, the morphology of the VPO catalyst should also shows a typical rosette-shape cluster (Taufiq-Yap *et al*, 2005; Taufiq-Yap *et al*, 2006; Taufiq-Yap and Saw, 2008). However, although the SEM pictures show similarity of the rosette shape cluster, the shape is more of a full bloom rose like structure.

This is due to the differences in preparation method used by those literatures and this project. The literatures mentioned above used dehydrate method in synthesizing their precursor. On the other hand, sesquihydrate method is used in synthesizing these precursors. This is in agreement with the SEM micrograph of a literature using the same precursor where they obtained a similar bloom rosette-shape (Leong *et al*, 2010). This bloom rosette-shape is predicted to have higher surface area which may leads to more active site for the catalytic reaction to takes place. (Leong *et al*, 2010). This prediction is in agreement with the BET surface area analysis result shown in table 4-3 where all the catalysts possess good surface area.

4.5.2 EDX

The table below shows the elements detected by the EDAX EDX analyser. The full analysis is attached as appendix.

Table 4-6: EDX elements identification

Catalyst	V At%	P At%	O At%	Cu At%	P/V	Cu/V
Bulk	19.12	21.84	59.04	0.00	1.1423	0.0000
0.1 % Cu	22.10	23.06	54.72	0.11	1.0434	0.0050
0.3 % Cu	19.84	20.69	59.30	0.17	1.0428	0.0086
0.5 % Cu	22.92	23.65	53.25	0.18	1.0318	0.0079

Based on Table 4-6, we can conclude that the element Vanadium, Phosphorus, Oxygen and Copper are presents in our catalyst. The atom percentage and P/V ratio expressed above only act as an indicator and doesn't reflect the actual sample composition of the entire bottle. This is because EDX sampling is performed on one of the VPO particle during SEM. There is a possibility that during the sampling, the particle being sampled doesn't contain the element that is desired such as copper in my case.

The existence of copper in the doped catalyst further proved the hypothesis in XRD where we deduce copper is either incorporated into the lattice of the VPO catalyst or too small amount to be detected by XRD. This is in agreement with the conclusion made in ICP OES analysis.

From the P/V ratio calculated, it can be seen that the undoped bulk catalyst is having a higher P/V ratio than the doped catalyst. This finding contradicts the ICP OES result where doped catalyst is found to have higher P/V ratio than undoped catalyst. This proves that EDX analysis is not suitable to be use for quantitative analysis as it doesn't reflects the overall composition of the catalyst.

CHAPTER 5

CONCLUSIONS AND RECOMMENDATION

5.1 Conclusions

Based on the results obtained through all the analysis performed, it is concluded that the addition of copper into the vanadium pyrophosphate catalyst might be a possible method to increase the activity and still maintain adequate selectivity for the conversion from *n*-butane to maleic anhydride.

The addition of copper increases the surface area of the catalyst from 0.1 % Cu to 0.3 % Cu. As surface area can be related to the activity where higher surface area means more active site for reaction to occur, we can assume that the higher the surface area, the better it is the activity of the catalyst.

The activity of the catalyst is also deduces to be high based on the V^{4+} and V^{5+} ratio. Both XRD and redox titration shows that the catalyst V^{4+} percentage is higher than the original bulk catalyst for 0.1 % Cu and 0.3 % Cu. Based on literature, the activity of the VPO catalyst is linked to the V^{4+} amount where higher V^{4+} catalyst commonly shows higher activity.

The selectivity of the catalyst is deduces based on the V^{5+} percentage in the catalyst. Based on redox titration data, copper doped catalyst achieved a V^{5+} percentage between the ranges of 14 % to 25 %. This amount of $V5^{+}$ is actually enough for an industrial usage catalyst as the main concern is still the conversion rather than the selectivity.

Although copper doped catalyst seems to give better catalytic performances with good conversion and selectivity, this concept is only valid with very low amount of dopant from 0.1 % Cu to 0.3 % Cu. The catalyst starts to behave differently when 0.5 % of copper is added in. The surface area actually decreases and the V^{4+} and V^{5+} trend changed from high V^{4+} and low V^{5+} to high V^{5+} and low V^{4+}.

5.2 Recommendations for further studies

The initial aim of this project is to study the catalytic performances of a copper doped VPO catalyst. However, due to technical issues and time constraints, the catalytic reaction analysis could not be performed.

Without the actual conversion and selectivity data from the reactor, the resulting performance of this catalyst is solely deduce based on literature and its physical and chemical properties. The deductions may not be correct and can be proven wrong. An opportunity is given to other students to further continue this research by running the catalytic reactor and interpreting the data to double confirm all the deduction made.

Another opportunity is that this research is performed using only three different samples with copper percentage ranging from 0.1% to 0.5%. Based on the results obtained, 0.3% copper addition is the optimum amount of copper that can give the best activity and selectivity. However, this can also be proven to be inaccurate as the changes in 0.5 % copper addition can be due to many errors from the precursor stage to the analysis stage. Also, 0.4% copper addition is not being analysed and this can be the actual optimum amount of dopant needed. Thus, the author invites other students to try out other ranges and double confirm the validity of his result.

REFERENCES

Abon, M., and Volta, J. C. (1997). Vanadium phosphorus oxides for *n*-butane oxidation to maleic anhydride. *Applied catalysis A: General* , 173-193.

Cornaglia, L., Irusta, S., Lombardo, E. A., Durupty, M. C., and Volta, J. C. (2003). The beneficial effect of cobalt on VPO catalysts. *Catalysis today* , 291-301.

Cranfield University. (2007). *Energy Dispersive X-ray Spectroscopy*. Retrieved from Cranfield University: http://www.cranfield.ac.uk/cds/cfi/eds.html

ENEA. (1992). *Replacement of Benzene with N-Butane in the production of Maleic anhydride.* Italy: UNEP IE.

Goh, C. K., and Taufiq-Yap, Y. H. (2007). Influence of Bi-Fe additive on properties of vanadium phosphate catalysts for *n*-butane oxidation to maleic anhydride. *Catalysis Today* , 408-412.

Govender, N., Friedrich, H. B., and Vuuren, M. J. (2004). Controlling factors in the selective conversion of *n*-butane over promoted VPO catalyst at low temperature. *Catalysis today* , 315-324.

I.Chorkendorff, J. (2003). *Concepts of Modern Catalysis and Kinetics.* Wiley-VCH.

ICB Chemical Profile. (2010, Feb 15). *Maleic Anhydride (MA) Uses and Market Data*. Retrieved from ICIS.com: http://www.icis.com/v2/chemicals/9076025/maleic-anhydride/uses.html

Ieda, S., Phiyanalinmat, S., Komai, S.-i., Hattori, T., and Satsuma, A. (2005). Involvement of active sites of promoted vanadyl pyrophosphate in selective oxidation of propane. *journal of catalysis* , 304-312.

IUPAC. (1985). IUPAC Recommendations Pure Applied Chemistry. 603.

IUPAC. (2005-2009). *doping in catalysis*. Retrieved Aug 8, 2010, from IUPAC GoldBook: http://goldbook.iupac.org/D01834.html

J.A. Moulijn, R. v. (1993). *CATALYSIS, An Integrated Approach to Homogeneous, Heterogeneous and Industrial Catalysis* . Elsevier Science.

Kung, H. H. (1994). Oxidative dehydogenation of light alkane. In D. D. Eley, *Advances in catalysis vol. 40* (p. 29). Elsevier.

Leong, L. K., Chin, K. S., and Taufiq-Yap, Y. H. (2010). The effect of Bi promoter on vanadium phosphate catalysts synthesized via sesquihydrate route. *Catalysis today* .

N., B., and F., C. (2006). VPO catalyst for *n*-butane oxidation to maleic anhydride: A goal achieved or a still open challenge? *Topics in Catalysis Vol 38* , 147-156.

Nagaraju, P., Lingaiah, N., Prasad, P. S., Kalevaru, V. N., and Martin, A. (2008). Preparation, characterisation and catalytic properties of promoted vanadium phosphate catalyst. *Catalysis communications* , 2449-2454.

Niwa, M., and Murakami, Y. (1982). Reaction mechanism of ammoxidation of toluene : IV. Oxidation state of vanadium oxide and its reactivity for toluene oxidation. *Journal of catalysis vol 76* , 9-16.

Radiological and Environmental Management. (2010, Nov 22). *Scanning Electron Microscope*. Retrieved from Purdue University: http://www.purdue.edu/rem/rs/sem.htm

Robinson, J. W. (2005). *Undergraduate instrumental analysis 6th Ed.* MARCEL DEKKER.

Samuel Roberts Noble Electron Microscopy Laboratory. (2010). *Elemental Identification*. Retrieved from University of Oklahoma: http://www.cranfield.ac.uk/cds/cfi/eds.html

Taufiq-Yap, Leong, & Hussien. (2004). Synthesis and characterisation of vanadyl pyrophosphate catalysts via vanadyl hydrogen phosphate sesquihydrate precursor. *Catalysis Today* , 715-722.

Taufiq-Yap, Y. H. (2006). Effect of Cr and Co Promoters Addition on Vanadium Phosphate Catalysts for Mild Oxidation of *n*-Butane . *Journal of natural gas chemistry* , 144-148.

Taufiq-Yap, Y. H., and Saw, C. S. (2008). Effect of different calcination environments on the vanadium phosphate catalysts for selective oxidation of propane and *n*-butane. *Catalysis Today* , 285-291.

Taufiq-Yap, Y. H., Goh, C. K., Waugh, K. C., and Kamiya, Y. (2005). Effect of Fe dopant on the physico-chemical and catalytic properties of vanadyl pyrophosphate catalysts. *React. Kinet. Catal. Lett.* , 271-278.

Taufiq-Yap, Y. H., Kamiya, Y., and Tan, K. P. (2006). Promotional Effect of Bismuth as Dopant in Bi-Doped Vanadyl Pyrophosphate Catalysts for Selective Oxidation of *n*-Butane to Maleic Anhydride . *Journal of Natural Cas Chemistry* , 297-302.

University of Oxford. (2010). *Basic operating principles of the Sorptomatic 1990.* Retrieved Aug 2, 2010, from The University of Oxford Surface Analysis Facility Web Site: http://saf.chem.ox.ac.uk/Instruments/BET/sorpoptprin.html

University, W. V. (2010). *Production of Maleic Anhydride.* Retrieved August 1, 2010, from West Virginia University: http://www.che.cemr.wvu.edu/publications/projects/large_proj/maleic.PDF

Vadim, V. G., and Moises, A. C. (2005). *Vanadium-Phosphorus-Oxides: from Fundamentals of n-Butane Oxidation to Synthesis of New Phases.* The Royal Society of Chemistry.

APPENDICES

APPENDIX A: Typical product distribution for alkane oxidation using three different catalysts

TABLE X

Typical Product Distributions for Alkane Oxidation on V–Mg Oxide ($Mg_3(VO_4)_2$ MgO), $Mg_2V_2O_7$, and VPO ($(VO)_2P_2O_7$)

Reactant	Reaction T (°C)	Alkane conv. (%)	Selectivity[a] (%)
	Over VPO catalyst		
C_3H_6	305	3.8	CO 12, CO_2 7, C_2H_4 81
C_3H_8	300	8	CO 62, CO_2 26, C_2H_4 4, C_3H_6 0, Ac 6, Ar 2
C_4H_{10}	300	7	CO 16, CO_2 10, C_2H_4 2, C_3H_6 1, Ac 7, Ar 2, MA 64
C_5H_{12}	325	7	CO 22, CO_2 15, MA 19, PA 44
	Over V–Mg–O catalyst		
C_2H_6	540	5.2	CO 28, CO_2 49, C_2H_4 24
C_3H_8	500	8.4	CO 14, CO_2 24, C_3H_6 62
iC_4H_{10}	475	4.0	CO 7, CO_2 22, C_4H_8 71
C_4H_{10}	475	4.1	CO 9, CO_2 22, C_4H_8 55, C_4H_6 14
cC_6H_{12}	484	8.4	CO 3, CO_2 14, C_6H_{10} 47, C_6H_6 36
	Over $Mg_2V_2O_7$ catalyst		
C_2H_6	540	3.2	CO 49, CO_2 21, C_2H_4 30
C_3H_8	475	10	CO 27, CO_2 18, C_3H_6 56
iC_4H_{10}	502	6.8	CO 39, CO_2 36, C_4H_8 25
C_4H_{10}	500	6.8	CO 33, CO_2 33, C_4H_8 31, C_4H_6 2

APPENDIX B: Calculation of dopant amount needed to be added into the VPO catalyst

Molecular weight of $VOPO_4.2H_2O$ is given as 197.94 g/mol

$$10 \text{ g of } VOPO_4.2H_2O = \frac{10\,g}{197.94\,g/mol} = 0.0505\,mol$$

For 0.1 mol% of dopant needed,

Dopant (mol) = 0.001 × 0.0505 mol = 0.0000505 mol

Total amount needed (g) = Molecular weight of dopant (g/mol) × 0.0000505 mol

Molecular weight of Copper nitrate = 241.6 g/mol

Thus,

$$241.6\,g/mol \times 0.0000505\ mol = 0.0122\ g$$

Table 5-1: Summary of mass of copper needed to be added into the catalyst

M.W.	mol %	mol	mass (g)
241.6	0.001	0.0505	0.0122
241.6	0.003	0.0505	0.0366
241.6	0.005	0.0505	0.0610

APPENDIX C: Crystallite Size measurement using powder XRD

Debye-Scherrer equation: $T(\overset{\circ}{A}) = \frac{0.89\lambda}{FWHM\cos\theta}$

Given λ of CuKα = 1.54 Å

FWHM (rad) = $FWHM(°) \times \frac{\pi}{180°}$

Data and calculation:

2 Theta	Theta (rad)	FWHM(')	FWHM(rad)	T(A)
bulk				
28.4109	0.2479	0.6271	0.0109	129.1766
22.7705	0.1987	1.3520	0.0236	59.2499
29.8960	0.2609	0.6262	0.0109	129.7989
0.1 Cu				
22.7967	0.1989	1.3109	0.0229	61.1104
28.4597	0.2484	0.6366	0.0111	127.2626
29.9530	0.2614	0.6236	0.0109	130.3574
0.3 Cu				
22.7323	0.1984	1.3028	0.0227	61.4834
28.4019	0.2479	0.6723	0.0117	120.4894
29.8924	0.2609	0.6677	0.0117	121.7304
0.5 Cu				
22.8274	0.1992	1.3329	0.0233	60.1050
28.4905	0.2486	0.7105	0.0124	114.0336
29.9822	0.2616	0.6979	0.0122	116.4872

APPENDIX D: XRD graphs and raw data

(Data included next page)

APPENDIX E: ICP-OES calculations

Converting mg/L to g/L: divide by 1000

Converting g/L to mol/L: divide by respective atomic weight of element

Data and calculation:

(Data included next page)

Sample	P mg/L	P g/L	P mol	V mg/L	V g/L	V mol	Dope mg/L	Dope g/L	Dope mol	P/V	Dope/V
Cu bulk	24.04	0.02404	0.00077616	30.81	0.03081	0.000604811	-	-	-	1.28	-
Cu 0.1	22.11	0.02211	0.000713848	27.04	0.02704	0.000530805	0.432	0.000432	6.79822E-06	1.34	0.013
Cu 0.3	19.61	0.01961	0.000633132	26.23	0.02623	0.000514904	0.467	0.000467	7.34901E-06	1.23	0.014
Cu 0.5	19.62	0.01962	0.000633455	24.19	0.02419	0.000474858	0.514	0.000514	8.08863E-06	1.33	0.017

Atomic weight of elements

P	30.973	g/mol
V	50.9415	g/mol
Cu	63.546	g/mol

APPENDIX F: Redox titration calculation

Calculation:

$V3+ = 0.2 (V1-V2+V3)$

$V4+ = 0.4V2-0.4V3-0.2V1$

$V5+ = 0.2V3$

Data and calculation:

bulk	initial	final	delta
KMnO4	4.5	15.2	10.7
	15.2	25	9.8
		V1	10.25
NH4Fe(II)SO4	5.4	17	11.6
	9.2	20.2	11
		V2	11.3
stage 2	initial	final	delta
	2	3.7	1.7
	3.7	5.3	1.6
			0
		V3	1.65
V4+	1.6		
V5+	0.33		
V av	4.1700		

0.1 Cu	initial	final	delta
KMnO4	1.4	11.7	10.3
	11.7	22.6	10.9
		V1	10.6
NH4Fe(II)SO4	10.1	21.3	11.2
	13.9	25.9	12
		V2	11.6
stage 2	initial	final	delta
	17.2	18.9	1.7
	19.6	21.5	1.9
		V3	1.80
V4+	1.9		
V5+	0.36		
V av	4.1593		

0.3 Cu	initial	final	delta
KMnO4	6	16.7	10.7
	16.7	27.2	10.5
		V1	10.6
NH4Fe(II)SO4	26.2	37.9	11.7
	21.3	33.6	12.3
		V2	12
stage 2	initial	final	delta
	21.3	23.2	1.9
	23.2	24.9	1.7
		V3	1.80
V4+	2.01		
V5+	0.36		
V av	4.1488		

0.5 Cu	initial	final	delta
KMnO4	15.5	24.8	9.3
	24.8	36	11.2
		V1	10.25
NH4Fe(II)SO4	10.7	22.2	11.5
	22.2	35	12.8
		V2	12.15
stage 2	initial	final	delta
	20.5	23.3	2.8
	23.3	26.2	2.9
		V3	2.85
V4+	1.67		
V5+	0.57		
V av	4.2522		

APPENDIX G: EDX analysis data

(Data included next page)